Sulphate Rotator Phases in Polarised Light

Roy Tärneberg

Department of Physics, Chalmers University of Technology, S-412 96 Göteborg

Z. Naturforsch. **51 a,** 1157–1160 (1996); received June 29, 1996

Li_2SO_4 has a well defined high-conducting fcc phase in the temperature range 577–860 °C, and $LiNaSO_4$ a bcc phase in the range of 518–614 °C. Both salts were studied in polarised light during sequences going from melt, through the cubic phase into the "room temperature" phase, and back to the cubic phase. The two cubic sulphate phases are compared with organic plastic rotator phases, especially regarding the formation of vapour snakes.

Key words: Plastic phases, rotator phases, vapour snake, lithium sulphate, lithium sodium sulphate

Introduction

Already in 1957 it was found that strong rotational oscillations must be expected for the high temperature modification of Li_2SO_4 (557–860 °C) [1]. In 1962 alternative models for the spatial orientation of the sulphate ions [2] were presented, and it was concluded from space considerations that the motion of the sulphate ions must be strongly coupled. Neutron powder diffraction studies in [3–5] showed that spherically symmetric sulphate ions are involved and confirmed the cubic framework of these ions. A single crystal neutron diffraction study of Li_2SO_4 gave much more detailed information concerning the cubic lattice and cation transport in Li_2SO_4 [6]. Brillouin and Raman scattering [7–11] also show clear indications of rotation or rotational vibrations of the sulphate ions.

Rotator Phases and Plastic Crystals

Studies of the rheological properties [12] of Li_2SO_4 have shown a resemblance to a group of organic materials called plastic crystals with properties similar to ideal crystals as well as liquids. These wax-like solids are normally optically isotrope. According to X-ray and neutron diffraction studies most of these crystalline materials have cubic structures. As a rule, the symmetry length of the crystal lattice is larger than the diameter of the molecules, which gives them enough space to rotate or oscillate in such "rotator phases" [13, 14].

The heat of melting ΔH_m is normally much larger than the enthalpy of any solid-solid phase transition ΔH_t. However, plastic crystals often have a larger latent heat for the solid-solid phase transition than for melting, see Table 1.

The two high-temperature phases of $LiNaSO_4$ and $LiAgSO_4$ have the same crystal structure, their ion transport properties are similar [15, 16] as well as their solid-solid transition enthalpies ΔH_t [17], see Table 1, and their enthalpies of melting ΔH_m.

A number of diffusion studies have been performed for organic plastic crystals [18] as well as for the sulphates [19]. Molecules diffuse in the first case while ions diffuse in the sulphates. In both cases the diffusion rates are higher and the activation energies lower than in "non-plastic" phases. Thus, for plastic cyclohexane the diffusion coefficient D is 10^{-7} cm^2/s at the melting point (7 °C) while D is often of the order of 10^{-11} cm^2/s for other organic solids. In the sulphate rotator phases they are of the order of 10^{-5} cm^2/s [19].

Another characteristic for plastic crystals is the phenomenon of forming a vapour snake [13, 14, 20]. When a sample is cooled from the melt, the small solidification enthalpy causes a quick crystallisation at the surface, where a crust of crystals is formed. Crystals are also formed along the cell walls. The thermal contraction will create a low-pressure bubble in the centre of the sample, underneath the crust. Evaporation will cause a local cooling of the substance and the crystallisation continues round the bubble. The crust will finally break and form a vertical funnel with small horizontal cracks in the centre of the salt column. To complete the comparison between the plastic crystals and the two sulphates, the formation of vapour snakes in Li_2SO_4 and $LiNaSO_4$ will now be studied.

Experimental

A furnace with two opposite glass windows was used. Two polaroid filters were mounted with perpendicular polarisation planes on either side of the furnace. The polarised light from the first filter was blackened out by the second filter. Only the glow from the

Reprint requests to R. Tärneberg.

0932-0784 / 96 / 1000-1157 $ 06.00 © – Verlag der Zeitschrift für Naturforschung, D-72072 Tübingen

Table 1. Transition temperatures and enthalpies for some compounds.

	Li_2SO_4	$LiNaSO_4$	$LiAgSO_4$	Na_2SO_4	AgI	N_2	CF_4	CCl_4
T_t	577	518	415	247	147	−237	−197	−48
T_m	860	614	570	884	555	−210	−183	−23
ΔH_t	24.8	24.7	28.3	6.5	6.25	0.23	1.48	4.6
ΔH_m	9.0	small	3.4	21.0	4.95	0.72	0.70	2.52
Phase	fcc	bcc	bcc	hex	bcc	hex	non-cub	fcc
Rotator	yes	yes	yes	no	no	yes	yes	yes

T_t = solid-solid transition (°C); T_m = melting temperature (°C); ΔH_t = transition enthalpy (kJ/mole); ΔH_m = enthalpy of melting (kJ/mole).

furnace enlightened the sample. In order to study the crystallisation process, the salt was first melted and then the temperature was lowered, passing the melt-solid temperature and the solid-solid transition temperature. The furnace was then switched on again and the temperature was raised to the vicinity of the melting point. Pictures were taken at every 50 °C or when a change in the crystal was seen.

Figure 1 A shows a sample of molten $LiNaSO_4$ at 900 °C. The polarised light is unaffected by the sample. Figure 1 B shows the same sample at 600 °C. The salt is now in the bcc phase. Small crystals have formed at the surface and are seen as a glow. The small spots are frozen air bubbles and the funnel in the centre is a vapour snake. Obviously, the cubic phase has no effect on the polarisation.

Results and Discussions

If the solidified sample was cooled slowly, the salt remained completely transparent (with exception of occasional tiny air bubbles) all the way down to the solid-solid phase transition, where it became opaque due to the formation of crystallites. Usually the tube cracked, see Fig. 2, but it did not fall apart if the salt column was reheated to the melting point. There were no visible changes at the phase transition, and the salt remained opaque until it started to melt.

Thus, one can distinguish between two states of the cubic sulphate: transparent or opaque, depending on the prehistory. It is obvious that the transparent mode is neither a single crystal nor amorphous. Instead, the plastic character allows gradual changes of the orien-

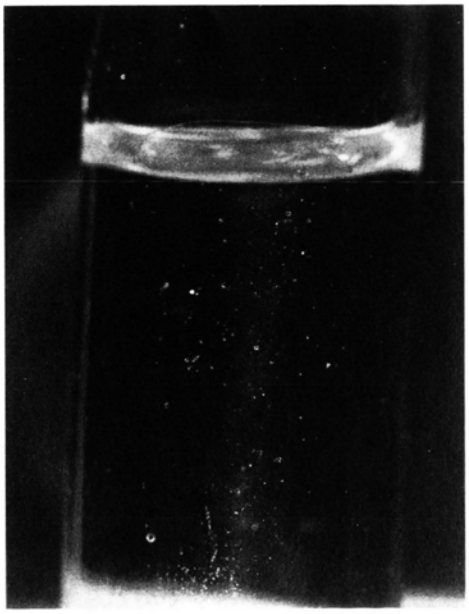

Fig. 1 A. $LiNaSO_4$ at 900 °C (molten phase).

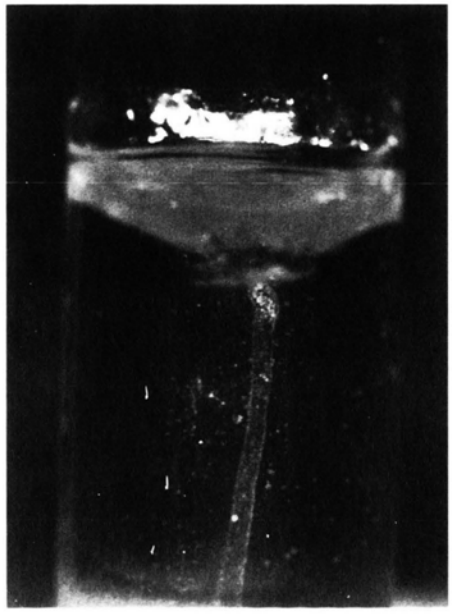

Fig. 1 B. $LiNaSO_4$ at 600 °C (solid phase, bcc).

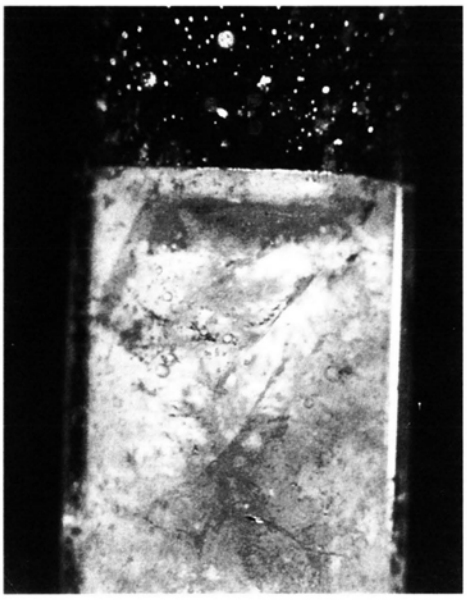

Fig. 2. Li_2SO_4 cooled below the solid-solid phase transition and then reheated to 600 °C.

tation of the crystal axes while the salt solidifies. However, once grain boundaries are formed, they remain until the melting point is reached.

It is likely that a vapour snake is formed if the cubic phase is cooled quickly. Figures 3A–3C show the formation of a vapour snake in $LiNaSO_4$. The crystallisation starts at the surface of the sample, Fig. 3A, it grows, Fig. 3B, and a small vertical funnel with horizontal cracks in all directions is formed in the middle of the column, Figure 3C. The sample remains homogenous and transparent except near the vapour snake.

The tendency to form vapour snakes is much stronger in $LiNaSO_4$ than in Li_2SO_4. This is expected since the heat of melting is much lower for bcc phases than for fcc phases, see Table 1. Of course, the formation is dependent on the heat transfer to the surroundings. Quick cooling immediately causes a vapour snake. We have found that if the cooling rate is rather slow, approx. 1 °C/min, this phenomenon can be avoided. Figure 4 shows a vapour snake in pure Li_2SO_4. This formation may occur also in the lower temperature range of the fcc phase, due to contraction. Normally the sample remains homogeneous between 860 and 800 °C.

The existence of vapour snakes can influence the results of some types of experiments. I do not expect that this is the case with conductivity measurements where the cooling rate is moderate. It is characteristic for diffusion experiments that the temperature between the melting and the annealing temperature is changed very quickly, which favours the growth of a vapour snake. Furthermore, the disturbances due to a vapour snake is largest in the upper part of the cell. Our diffusion experiments were performed in quartz

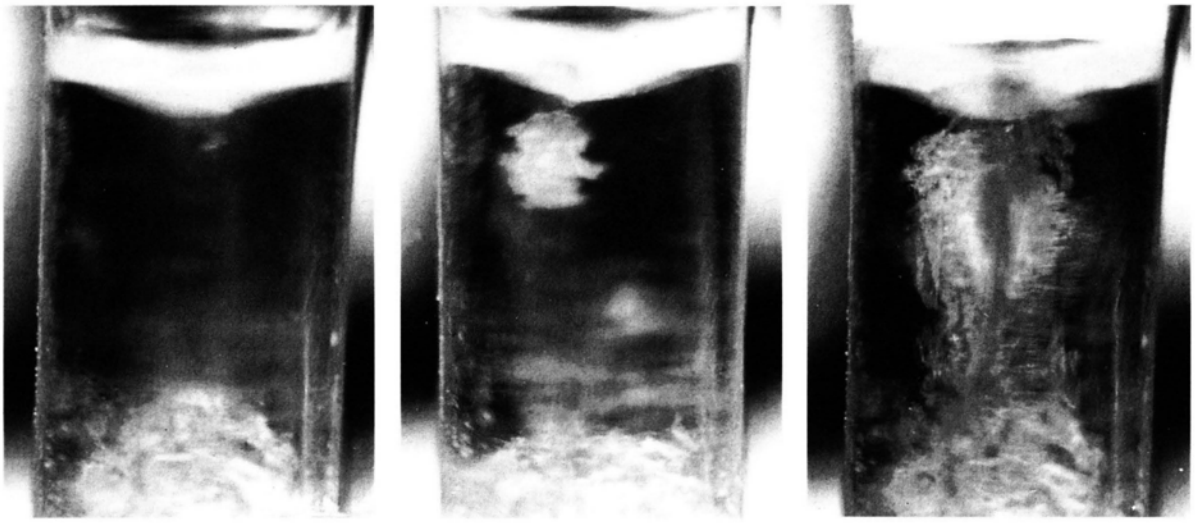

a b c

Fig. 3A–3C. The birth and development of a vapour snake in $LiNaSO_4$.

Fig. 4. A vapour snake in pure Li_2SO_4 at 800 °C.

glass tubes. Especially for $LiNaSO_4$ a large percentage of the measurements had to be rejected. The presence of vapour snakes was detected by the received nonexponential data, especially from the upper part of the sample. To lower the cooling rate at the melt-solid transition, we found it important to cover the sample with a large steel block in the furnace, which also stabilised the temperature round the sample.

Conclusion

My study has, inter alia, demonstrated a similarity between molecular and ionic plastic phases regarding the occurrence of vapour snakes. Vapour snakes can cause a strong enhancement of the "as-measured" diffusion coefficients in cases where transport along high diffusivity paths is more important than bulk diffusion.

This study has also shown that the grain boundaries do not vanish at the solid-solid transition temperature when the temperature is raised from the solid opaque phase to the cubic phase.

[1] T. Førland and J. Krogh-Moe, Acta Chem. Scand **11,** 565 (1957).
[2] H. A. Øye, Thesis, The Technical University of Norway (1963).
[3] L. Nilsson, J. O. Thomas, and B. C. Tofield, J. Phys. C: Solid State Phys. **13,** 6441 (1980).
[4] L. Nilsson, N. H. Andersen, and J. K. Kjems, Solid State Ionics **6,** 209 (1982).
[5] L. Nilsson, N. H. Andersen, and A. Lundén, Solid State Ionics **34,** 111 (1989).
[6] R. Kaber, L. Nilsson, N. H. Andersen, A. Lundén, and J. O. Thomas, J. Phys.: Condens. Matter. **4,** 1925 (1992).
[7] R. Aronsson and L. M. Torell, Phys. Rev. B **36,** 4926 (1987).
[8] R. Aronsson, L. Börjesson, and L. M. Torell, Phys. Lett. **98A,** 205 (1983).
[9] L. Börjesson and L. M. Torell, Proc.-Electrochem. Soc. **86-1** (Molten Salts), 21.
[10] L. Börjesson and L. M. Torell, Solid State Ionics, **18/19,** 582 (1986).
[11] L. Börjesson and L. M. Torell, Phys. Rev. B **32,** 2471 (1985).
[12] B. Jansson and C.-A. Sjöblom, Rheol. Acta **16,** 628 (1977) and **20,** 360 (1981).
[13] D. Schmid and U. Wannagat, Chemiker Z. **98,** 575 (1974).
[14] D. Schmid, Chemiker Z. **99,** 12 (1975).
[15] A. Lundén, Materials for Solid State Batteries, p. 149, (Ed. B. V. R. Chowdari and S. Radhakrishna World Scientific Publ. Co, Singapore 1986).
[16] A. Lundén, in Fast Ion Transport in Solids, eds. B. Scrosati, A. Magistris, C. M. Mari and G. Mariotto, NATO ASI Series E: **250,** 181 (1993) (Kluwer Academic Publ., Dordrecht).
[17] G. Petit and C. Bourlange, Compt. Rend. Acad. Sci. Paris **245,** 1788 (1957).
[18] A. V. Chadwick and J. N. Sherwood, Diffusion Processes, Vol. 2, p. 475, Eds. J. N. Sherwood, A. V. Chadwick, W. M. Muir, and F. L. Swinton, Gordon & Breach, London 1971.
[19] R. Tärneberg and A. Lundén, Solid State Ionics, submitted to be published (1996).
[20] M. K. Phibbs and H. I. Schiff, J. Chem. Phys. **17,** 843 (1949).

Verantwortlich für den Inhalt: A. KLEMM
Satz und Druck: Konrad Triltsch, Würzburg